CORE
Metadata, citation and similar papers at core.ac.uk
Provided by idUS. Depósito de Investigación Universidad de Sevilla

EVALUATION OF GENERALIZED STRESS INTENSITY FACTORS IN ANISOTROPIC ELASTIC MULTIMATERIAL CORNERS.

A. Barroso, P. Toro, V. Mantič and F. París

School of Engineering, University of Seville, Camino de los Descubrimientos s/n, E-41092 Sevilla, Spain.

ABSTRACT

A least squares method has been developed to evaluate Generalized Stress Intensity Factors (GSIF) in 2D anisotropic linear elastic multimaterial corners. As characteristic exponents (order of stress singularities) and characteristic angular functions are evaluated first in a semi-analytical way, the only parameters to adjust in the least squares procedure are the GSIFs. Numerical examples are presented involving single and bi-material isotropic free-free corners for comparison purposes with other authors. The Boundary Element Method (BEM) has been used for numerical solutions of the presented problems. Although the procedure is tested in the present work, only with single and bimaterial isotropic free-free corner configurations, due to the easier possibility to compare with solutions of these problems by other authors, the proposed method is valid for any generic multimaterial corner configuration involving homogeneous anisotropic linear elastic materials.

1. INTRODUCTION

Assuming linear elasticity, and considering a polar coordinate system (r,θ) with its origin at the corner tip, the 2D asymptotic stress field at the neighbourhood of the apex of a re-entrant corner composed by one or more materials (Fig. 1), is unbounded as r→0 and can be expressed in a series expansion form, see Eq. (1).

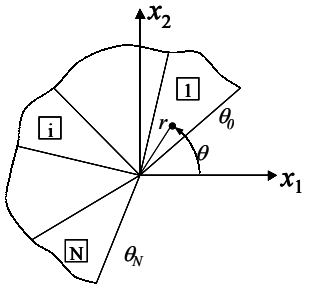

Fig. 1. *N*-material corner.

$$\sigma_{ij}(r,\theta) \approx \sum_{k=1}^{K} \frac{K_k}{r^{1-\lambda_k}} f_{ijk}(\theta)\,, \quad (i,j=r,\theta). \tag{1}$$

where λ_k are the orders of stress singularity ($0<\lambda_k<1$), $f_{ijk}(\theta)$ are angular functions of the polar coordinate θ, smooth inside each material, and K_k are the generalised stress intensity factors (GSIFs in what follows). A complete characterisation of this singular stress field is achieved through the knowledge of λ_k, $f_{ijk}(\theta)$ and K_k for the terms considered in the asymptotic series expansion.

The order of stress singularities λ_k and the structure of the angular function $f_{ijk}(\theta)$ only depend on the local properties of the corner (material properties, geometry and boundary conditions at the corner), while the GSIFs are global dependent, being then necessary for their calculation the knowledge of the far field loading and geometry. The local nature of the order of stress singularities and characteristic angular functions implies that they can be re-used in any problem having the same local corner configuration while the results for GSIFs are only valid for a particular geometry and loading. Additionally, evaluation of a GSIF requires in general the use of a numerical or experimental method. This fact may be the reason why there are more papers devoted to finding order of stress singularities rather than to finding GSIFs.

As calculation of GSIFs typically involves the use of numerical models and postprocessing of the results, the final accuracy of results is highly dependent on the methods applied at both stages. Due to the singular asymptotic character of the stress field, the numerical analysis and the postprocessing operations have to be performed with care. GSIFs extracted from remote data may not represent the assumed asymptotic field while GSIFs extracted from too-near corner tip data may be perturbed by possibly large discretization errors near the corner tip. Several approaches have tried to overcome these difficulties, e.g. "reciprocal work integral contour method", based on Betti's reciprocal law, see for example recent works by Banks-Sills and Sherer [1], Qian and Akisanya [2] and Wu [3] amongst others.

The objective of this work is to present a simple procedure for a reliable evaluation of GSIFs in multimaterial corners with any kind of homogeneous linear elastic materials, using a postprocessing technique which is, in some sense, optimal.

2. ORDER OF STRESS SINGULARITIES

Several studies have been devoted to the evaluation of the order of stress singularities for different geometries and material properties, using different techniques. At present moment, and considering multimaterial corners characterized by: homogeneous linear elastic materials in each wedge, perfect adhesion between wedges, homogeneous boundary conditions and plane states (plane stress, plane strain or generalized plane strain), it can be certainly said that it is not difficult to obtain accurate values for the order of stress singularities and characteristic angular functions (under the above considerations), see for example the works of Dempsey and Sinclair [4,5], Pageau et al. [6,7], Ting [8], Mantič et al. [9], Poonsawat et al. [10,11] and Barroso et al. [12] amongst others.

In this work the orders of stress singularities and characteristic angular functions have been obtained from a previous work of the present authors, Barroso et al. [12], a general anisotropic elastic behaviour being allowed (non-degenerate and degenerate materials in the framework of Stroh formalism of anisotropic elasticity). The calculations are semi-analytical (numerical calculations are only applied in the evaluation of roots of analytic functions), giving rise to accurate results which were successfully tested with previous works by other authors.

3. GENERALIZED STRESS INTENSITY FACTORS

The coefficients of the asymptotic expansion can be evaluated using different post-processing techniques, see Helsing and Jonsson [13] for a comprehensive review. In all cases numerical or experimental data are needed, and typically, the accuracy of GSIFs compared to the accuracy that can be achieved in computing λ_k and $f_{ijk}(\theta)$ is often substantially worst. Some interesting comments, regarding the validity and accuracy of numerical results presented in literature, can be seen in Helsing and Jonsson [14].

In the present work BEM models have been employed as the numerical tool for the evaluation of the GSIFs due to the high accuracy of the boundary and interface data obtained by this method.

4. LEAST SQUARES PROCEDURE

In this work a least squares method has been employed in a similar way as in Munz and Yang [15] using the boundary values of $u_r(r,\theta)$ and $u_\theta(r,\theta)$ at the external faces (θ_0, θ_N) and interfaces between the wedges (θ_i, i=1,...,N-1) in the case of multimaterial corners, see Fig. 1. An error function J is defined as:

$$J(K_1,...,K_k)=\sum_{\alpha=1}^{2}\sum_{j=0}^{N}\sum_{n=1}^{M}\left[u_\alpha^{num}(r_n,\theta_j)-u_\alpha^{series}(r_n,\theta_j,K_1,...,K_k)\right]^2 \quad (2)$$

where the sum of quadratic errors between the numerical solution $u^{num}(r,\theta)$ and the series expansion approximation $u^{series}(r,\theta,K_1,...,K_k)$ is extended to both in-plane components u_r (α=1) and u_θ (α=2), the N+1 faces/edges (θ_0,..., θ_N) of the N-material corner, and the group of M nodes at each edge. The set of optimal values for K_i (i=1,...,k) is obtained when satisfying the following system of linear equations:

$$\frac{\partial J(K_1,...,K_k)}{\partial K_i}=0\,,\ (i=1,...,k) \quad (3)$$

The accuracy of the results for the GSIFs will be greatly conditioned by the quality of the mesh as well as by the set of nodes chosen for the least squares adjustment. It would be desirable that accurate results were as less dependent as possible on the group of nodes selected.

5. NUMERICAL EXAMPLES

Two problems found in literature have been analysed in order to see the accuracy of the present method: a single homogeneous isotropic free-free corner configuration and a bimaterial free-free isotropic corner configuration.

5.1. THE 90º NOTCH PROBLEM

The first problem is a 90º notch specimen of a single homogeneous isotropic material, which has been analysed in two steps. A first step in which the asymptotic solution for an opening mode of a free-free isotropic corner has been applied at the remote boundaries, in order to test the overall accuracy of the method. In this problem the local solution is extended to the entire domain and only discretization errors should be expected. A second step has been conducted to see the accuracy of the procedure in a more realistic problem in which a far field tensile loading is applied at the upper and lower boundaries. In this problem the asymptotic solution is not valid far from the notch tip.

5.1.1. SINGLE TERM LOCAL SOLUTION IN THE WHOLE DOMAIN

The geometry that has been first used to check the procedure is a single notched specimen taken from the work of Helsing and Jonsson [13], shown in Fig. 2. Values of a/w=0.5 and h/w=1 have been taken, a being 5cm. The BEM model has 709 nodes and 709 linear elements, the size of the elements being 0.1 cm at horizontal and vertical faces. In the two faces converging at the notch tip, the size of the elements increases from 10^{-7} cm at the notch tip with a factor of 1.5 until a length of 0.1 cm is reached, the rest of elements of the face having a constant length equal to 0.1 cm. Each one of these faces has 100 elements. A detail of the BEM mesh at the notch tip is shown in Fig.3.

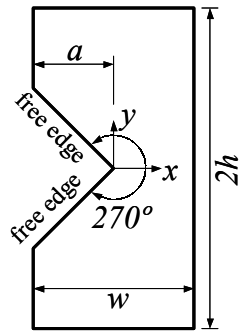

Fig. 2. The 90º notch specimen (Ref.[13]).

In order to first check the numerical accuracy of the procedure, including the numerical solution and the postprocessing using expressions (2) and (3), analytical expressions of the free-free wedge stresses in a single-term pure opening mode were applied at the boundary of

the specimen shown in Fig. 2. Each one of the terms of the asymptotic linear elastic solution at the corner tip, for an opening (or symmetrical) mode, is given by expressions (4a-4c) for stresses and (4d-4e) for displacements (taken from the work of Seweryn and Molski [16]), where λ are the roots of the characteristic determinant of the corner problem and $K_I(\lambda)$ are the corresponding GSIF associated to these roots λ.

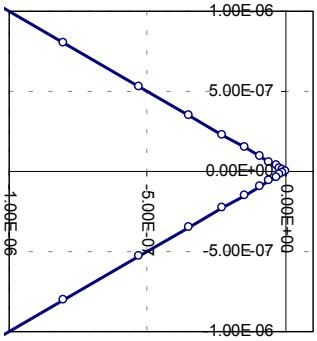

Fig. 3. Detail of the BEM mesh at the notch tip.

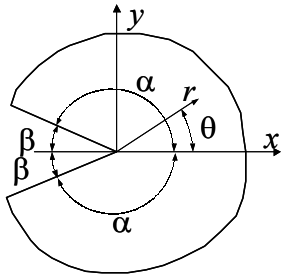

Fig. 4. Angle definitions.

$$\sigma_r = \frac{K_I(\lambda)}{(2\pi r)^{1-\lambda} C_1}\left(\frac{3-\lambda}{1+\lambda}\cos[(1+\lambda)\alpha]\cos[(1-\lambda)\theta] + \cos[(1-\lambda)\alpha]\cos[(1+\lambda)\theta]\right) \quad (4a)$$

$$\sigma_\theta = \frac{K_I(\lambda)}{(2\pi r)^{1-\lambda} C_1}\left(\cos[(1+\lambda)\alpha]\cos[(1-\lambda)\theta] - \cos[(1-\lambda)\alpha]\cos[(1+\lambda)\theta]\right) \quad (4b)$$

$$\tau_{r\theta} = \frac{K_I(\lambda)}{(2\pi r)^{1-\lambda} C_1}\left(\frac{1-\lambda}{1+\lambda}\cos[(1+\lambda)\alpha]\sin[(1-\lambda)\theta] - \cos[(1-\lambda)\alpha]\sin[(1+\lambda)\theta]\right) \quad (4c)$$

$$u_r = \frac{K_I(\lambda)}{(2\pi r)^{1-\lambda} 2\mu\lambda C_1}\left(\frac{3-\lambda-4\nu}{1+\lambda}\cos[(1+\lambda)\alpha]\cos[(1-\lambda)\theta] + \cos[(1-\lambda)\alpha]\cos[(1+\lambda)\theta]\right) \quad (4d)$$

$$u_\theta = \frac{-K_I(\lambda)}{(2\pi r)^{1-\lambda} 2\mu\lambda C_1}\left(\frac{3+\lambda-4\nu}{1+\lambda}\cos[(1+\lambda)\alpha]\sin[(1-\lambda)\theta] + \cos[(1-\lambda)\alpha]\sin[(1+\lambda)\theta]\right) \quad (4e)$$

where $C_1 = \cos[(1+\lambda)\alpha] - \cos[(1-\lambda)\alpha]$, $\mu = \frac{E}{2(1+\nu)}$, E is the Young modulus, ν is the Poisson ratio and the angle α is defined in Fig. 4.

According to (4b) and (4c) the stress vector at the inclined faces is null. The analytical value of K_I introduced in the above expressions was K_I=1. The least squares adjustment has been performed using all combinations of consecutive node groups between the first node beside the tip (node 1) and the last node of the inclined face (node 100) with a total of 5000 combinations (100×100/2). The absolute value of the relative errors obtained for K_I is shown in Fig. 5 (given in %).

In Fig. 5, the right axis represents the initial node number of the group of nodes, the left axis the final node number of the group, the z coordinate being the relative error (absolute value in %) with a cut at 2% (the half bottom part of Fig. 5 is not feasible).

From Fig. 5, as could be expected, the only origin of significant errors appear when considering, for the least squares adjustment, only groups of a few nodes adjacent to the tip of

the corner due to discretization errors of the BEM model as r→0. As the boundary loadings correspond to a pure mode I, no boundary effects are found when approaching the remote nodes and errors decrease as soon as the groups of nodes are far from the tip, or they include nodes far from the tip, these errors being below 0.5 % for almost all combinations.

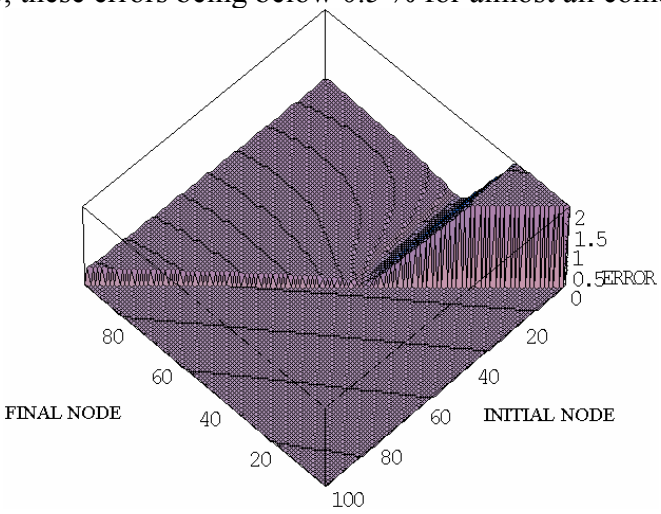

Fig. 5. Errors in K_I in a pure opening mode.

5.1.2. FAR-FIELD TENSILE LOADING

Let us now consider the same problem shown in Fig. 2, now subjected to tensile loadings. This problem was studied in detail by Helsing and Jonsson [13]. The geometry and the applied loads induce an opening mode at the tip of the notch. Using the same mesh as in the previous case, the use of formulas (2) and (3) considering a different number of terms of the asymptotic expansion leads to the results shown in Figs. (7a) to (7d). These figures show the absolute value of the relative error (in %) for K_I when using three, five, seven and nine terms of the series expansion respectively in Fig. 7a, b, c and d. Attention should be paid to the fact that the horizontal axes represent node numbers and not distances from the notch tip, with such a graphical representation (distances instead of node numbers), the peak at the right hand side of graphs in Figs. 7 would concentrate much more at this side of the figures as the length of these elements is much shorter. It is also remarkable in these figures the higher dependency in the error value with the last node number (the direction of the highest slope), at least in the right hand side of the figures.

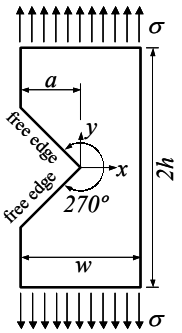

Fig. 6. Tensile loading on the 90º notched specimen (Ref.[13]).

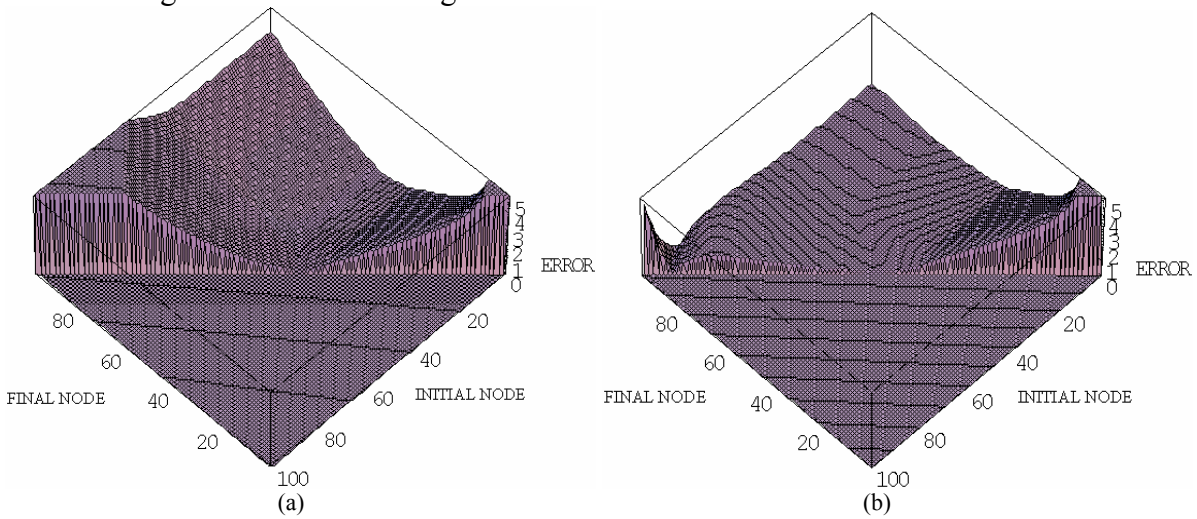

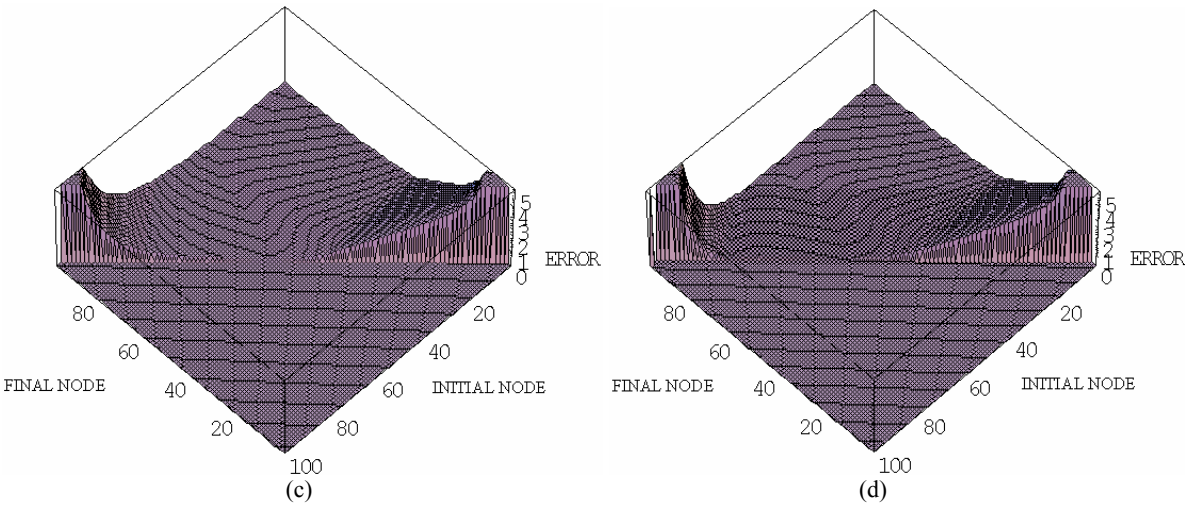

Fig. 7. Errors in K_I (in %) using (a) three, (b) five, (c) seven and (d) nine terms in the series expansion.

In the above figures, a value of K_I=4.295886967699 has been taken from Helsing and Jonsson [13] as the theoretical correct value. It can be appreciated in Figs. 7 that the more terms are considered in the least squares procedure, the more accurate is the value of K_I for more "group of nodes". As mentioned before, the errors for short groups of nodes very near to the corner tip are higher due to higher discretization errors of the BEM results there, and appear at the right hand side of graphs in Figs. 7. Higher errors associated to the use of short group of nodes which are far enough from the notch tip appear because of the non-validity of expression (1) near the left vertical edges of the specimen (see Fig. 6), they appear at the left hand side of graphs in Figs. 7.

From Fig. 7a it can be seen that a very good agreement in the value of K_I (from an engineering point of view, errors below 1 or 2%) is possible (by the present method) for several "windows=group of nodes" in the least squares adjustment, even more if the graphical representation with distances, and not with node numbers, is used. As additional terms of the series expansion are introduced in the representation of stresses and displacements, the number of windows in which the error is low, is much larger. It has been obtained, for example in Fig. 7d with nine terms, reasonable low errors for practically all "reasonable" windows. Only at the extreme-right hand side and extreme-left hand side of the Fig. 7d, which represents a few group of nodes very near and very far from the notch tip with very few nodes, higher errors are obtained. The accuracy of the least squares procedure has been tested using expressions (2) and (3) for either one or more edges (with artificial radial lines of interior points in the BEM model) considering either one or both components of displacements. The results indicated that the more information is introduced in (2), the more accurate is the final result. The results in Figs. 7, correspond to calculations including both edges of the notch with both displacement components $u_\alpha(r,\theta_0)$ and $u_\alpha(r,\theta_1)$, with $\alpha = r,\theta$.

5.2. BIMATERIAL CORNER

The procedure developed was also checked with the problem of a bi-material wedge, shown in Fig. 8, taken from the work of Qian and Akisanya [2]. The numerical solution given in the paper by Qian for this bi-material notch is obtained for the following Dundur's parameters: α=0.8, β=0.2 (which correspond to a situation in which the material at the upper part of the specimen in Fig. 8 is approximately ten times stiffer than the other).

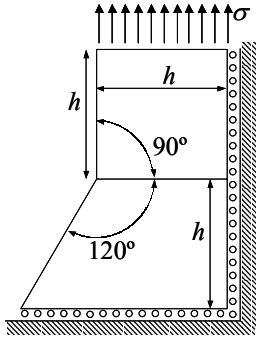

Fig. 8. Bimaterial corner (Ref.[2])

For this particular configuration three real characteristic exponents λ_i (i=1,2,3) where obtained $\lambda_1 = 0.6747$, $\lambda_2 = 1.1637$ and $\lambda_3 = 1.5938$, only the first characteristic exponent leads to singular values of stresses when $r \to 0$. The expressions for stresses and displacements used by Qian and Akisanya [2] are:

$$\sigma_{ij}^{m}(r,\theta) = \sum_{k=1}^{N} H_k \, r^{\lambda_k - 1} \, f_{ijk}^{m}(\theta) \qquad u_i^{m}(r,\theta) = \sum_{k=1}^{N} H_k \, r^{\lambda_k} \, g_{ik}^{m}(\theta) \tag{5}$$

$$H_k = \sigma \cdot h^{1-\lambda_k} a_k(\alpha, \beta, \lambda_k, \theta_1, \theta_2) \tag{6}$$

where m is the material, H_k is the GSIF associated to the characteristic exponent λ_k, a_k is adimensional, and the functions f_{ijk}^{m} and g_{ik}^{m} are known explicit expressions in terms of elastic material properties, the polar coordinate θ, the angles θ_1 and θ_2, and the characteristic exponent λ_k, see Qian and Akisanya for further details [2].

The coefficients a_k presented by Qian and Akisanya have been obtained using a theoretically path-independent contour integral (finally transformed into a domain integral using Gauss's theorem). It has been shown numerically that this integral is reasonably path-independent when evaluated at three different distances from the notch tip: 0.0053h-0.0063h, 0.0217h-0.0255h and 0.0869h-0.11h. The mean values of these coefficients a_k (in the above three domains and in adimensional form) are: $a_1 = 0.6301$, $a_2 = -0.3671$, $a_3 = 0.5443$. The dependency of the values of a_k obtained using the least squares procedure can be expected to be as slight as the variation for K_I shown in Fig. 7d, if enough terms in the asymptotic expansion of the near-tip corner solution are considered and a reasonable choose of the window is made.

The BEM model applied is represented in Fig. 9 in undeformed and deformed configurations, scaling factor being used for the displacements obtained by the BEM model.

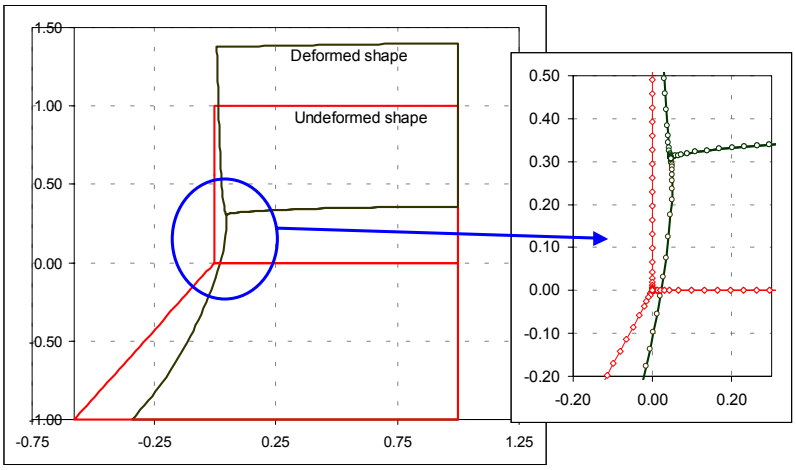

Fig. 9. Deformed and undeformed shapes of the BEM model.

With a length of $10^{-8}h$ used at the adjacent element to the notch tip and a length of 0.025h used far from the tip, a factor of 1.5 was used to increase the length of the elements from the tip to the outer boundary (up to a length of 0.025h). Linear elements were employed and a total of 66 elements exist at θ=0º and θ=90º while up to 72 elements are placed at θ=-120º.

For an accurate determination of the first coefficients H_k, it is necessary to use in the series expansion expressions in (5) some additional terms to the number of H_k searched. Using the

computational tool developed in Barroso et al. [12] the three first real characteristic exponents λ_k have been calculated, showing slight differences from those presented in Qian and Akisanya. These values are: $\lambda_1 = 0.673473$, $\lambda_2 = 1.167477$ and $\lambda_3 = 1.589147$. The next in-plane characteristic exponents, also obtained in this work, are complex conjugate $\lambda_4 = 2.88716 \pm 0.5731i$. The determination of the first coefficient H_1 was made taking into account the three terms associated to the real characteristic exponents.
The values obtained for a_1 (equal to H_1 if σ=1 and h=1) adjusting with all possible windows are presented in Fig. 10a with a range of values in the z-axis of (0, 1) and in Fig. 10b with a zoom in this z-axis range between (0.6, 0.8).

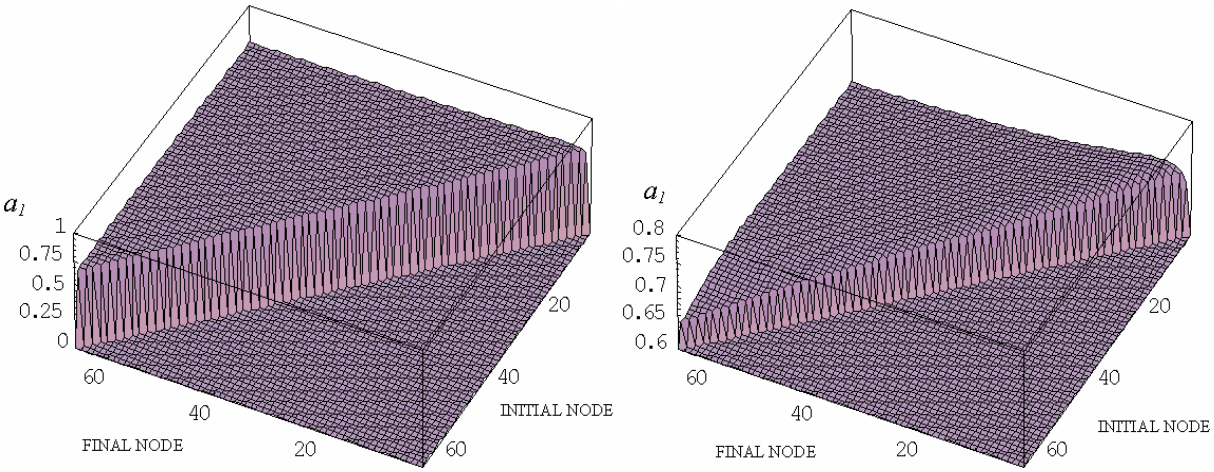

Fig. 10. Values of a_1 for the bimaterial problem.

From Fig. (10b) it can be seen that the largest variations of K_I appear as the groups of few nodes approach either the tip (right hand side of the figure) or the outer boundary (left hand side of the figure).

Using both u_r and u_θ at the three faces (θ=-120º, 0º and 90º) and considering a group of 40 nodes from node 15 (r= $5.818585 \cdot 10^{-6}$ h) to node 55 (r= 0.6224868 h) in the flattest part of the surface in Fig. 10b, the value for the first coefficient is a_1=0.673688 (the other two calculated coefficients, a_2 and a_3, should not be considered here as reference values unless other terms are included in the series expansion. In any case, the values obtained for these coefficients are a_2=-1.71057 and a_3=0.807724, which greatly differ from those obtained in Qian's work. The displacement component u_r from the numerical BEM model, as well as the series expansion expressions using the obtained values of λ_k and H_k (or a_k) in this work and in Qian's work [2] are graphically presented in Fig. 11 along θ=-120º in log-log scale for h=1.

As the coefficients a_k (k=1,2,3) have been obtained through a least squares technique from node 15 (r= $5.818585 \cdot 10^{-6}$) to node 55 (r= 0.6224868), it can be appreciated in Fig. 11 that, as expected, an excellent agreement is achieved between BEM results and series expansion results in this region. Outside this region, and due to the fact that 40 (out of 66) nodes have been used in the adjustment, also very good results are obtained at small and large distances (radius), greatest differences appearing only near the outer boundary.

Results by Qian and Akisanya [2] were obtained from a FEM model and an excellent agreement was reported in the radius range from $10^{-4}h$ to$10^{-1}h$. In Fig. 11 this agreement is also very good compared to the BEM results at this range, but higher differences are observed outside this range.

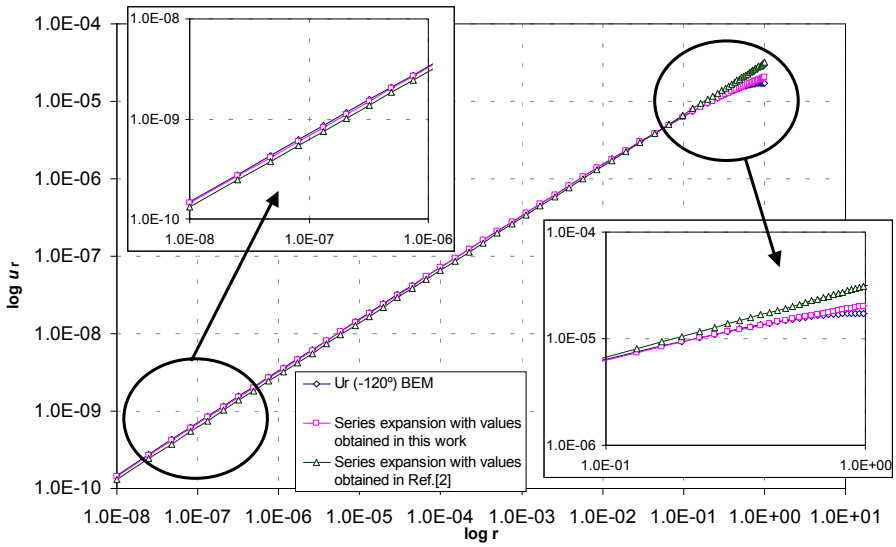

Fig. 11. log-log representation of u_r component along θ=-120º face.

The difference in the values of a_1 between Qian's mean value (0.6301) and the one obtained in this work (0.6782) is approximately of a 7%. The huge differences between the other two coefficients should not be taken into account for comparison, as mentioned before, unless additional terms are considered in the series expansion. Unlike the habitual good agreements in literature for characteristic exponents λ_k using various approaches, greater differences often appear when comparing GSIF values. As mentioned earlier, very interesting remarks regarding this lack of accuracy can be found in Helsing and Jonsson [14].

From the author's point of view, comparisons for GSIF values are often very tedious due to the different GSIF structure used by each author. Interesting attempts of standardized structures for the GSIF coefficients have been presented by Pageau et al. [17].

6.- CONCLUSIONS

A procedure for calculating Generalized Stress Intensity Factors (GSIF) in 2D multimaterial corners involving any kind of homogeneous anisotropic linear elastic materials is presented. The materials are considered perfectly bonded at common interfaces and with homogeneous boundary conditions at the external faces. Also corners with all materials bonded can be considered. The procedure is based on a least squares fitting of an asymptotic series expansion of displacements and displacements obtained by a BEM model.

Using a previous work of the authors for the evaluation of characteristic exponents and characteristic angular functions in these kind of corners, Barroso et al. [12], all the effort in the least squares adjustment is focused on the GSIF coefficients evaluation. Different numerical examples of 2D elastic corners having analytical "handy-solutions" involving one or two materials have been performed. Comparisons of the results with the first benchmark problem is excellent while some differences appear in the other problem.

As mentioned in other works, a larger number of high accuracy solutions of benchmark problems, is clearly needed, in order to compare new procedures with confidence, as done in Helsing and Jonsson [13], and in Banks-Sills and Sherer [1]. Additionally, the different standardization procedures used by different researchers implies a great effort for comparison purposes, this fact implies a necessity for a generally accepted normalization procedure for the GSIF coefficients, following for instance the line proposed by Pageau et al. [17].

This work is in the framework of the actual research of the authors in the mechanical characterization of multimaterial corners which typically appear in metal to composite adhesively bonded joints, see references [18,19]. Once the stress field is evaluated completely at these points and experimental test are performed, failure predictions from a Fracture Mechanics point of view, based on these results, can be attempted.

ACKNOWLEDGMENTS

The authors gratefully acknowledge the financial support of the Spanish Ministry of Science and Technology (project MAT2003-03315).

References

1. **Banks-Sills, L.** and **Sherer, A.**, "A conservative integral for determining stress intensity factors of a bimaterial notch", *Int. J. Fracture* **115** (2002), 1-26.
2. **Qian, Z.Q.** and **Akisanya, A.R.**, "Wedge corner stress behaviour of bonded dissimilar materials", *Theor. Appl. Fract. Mec.*, **32** (1999), 209-222.
3. **Wu, K.C.**, "Near-tip field and the associated path-independent integrals for anisotropic composite wedge", *The Chinese Journal of Mechanics*, **17**/1 (2001), 21-28.
4. **Dempsey, J.P.** and **Sinclair, G.B.**, "On the stress singularities in the plane elasticity of the composite wedge", *J. Elasticity*, **9**/4 (1979), 373-391.
5. **Dempsey, J.P.** and **Sinclair, G.B.**, "On the singular behaviour of a bi-material wedge", *J. Elasticity*, **11**/3 (1981), 317-327.
6. **Pageau, S.S., Joseph, P.F.** and **Biggers, Jr., S.B.**, "The order of stress singularities for bonded and disbonded three-material junctions", *Int. J. Solids Struct.*, **31** (1994), 2979-2997.
7. **Pageau, S.S.** and **Biggers, Jr., S.B.**, "A finite element approach to three-dimensional singular stress states in anisotropic multimaterial wedges and junctions", *Int. J. Solids Struct.*, **33** (1996), 33-47.
8. **Ting, T.C.T.**, "Stress singularities at the tip of interfaces in policristals", *Damage and Failure of Interfaces* (Ed. by Rossmanith). Balkema, Rotterdam (1997), 75-82.
9. **Mantič, V. París, F.** and **Cañas, J.**, "Stress singularities in 2D orthotropic corners", *Int. J. Fracture* **83** (1997), 67-90.
10. **Poonsawat, P., Wijeyewickrema, A.C.** and **Karasudhi, P.**, "Singular stress fields of an anisotropic composite wedge with africtional interface", *ASCE 12th Engineering Mechanics Conference*, La Jolla, San Diego, CA (1998), 578-581.
11. **Poonsawat, P., Wijeyewickrema, A.C.** and **Karasudhi, P.**, "Singular stress fields of angle-ply and monoclinic bimaterial wedges", *Int. J. Solids Struct.*, **38** (2001), 91-113.
12. **Barroso, A., Mantič, V.** and **París, F.**, "Singularity analysis of anisotropic multimaterial corners", *Int. J. Fracture*, **119**/1 (2003), 1-23.
13. **Helsing, J.** and **Jonsson, A.**, "On the computation of stress fields on polygonal domains with V-notches", *Int. J. Numer. Meth. Eng.*, **53** (2002), 433-453.
14. **Helsing, J.** and **Jonsson, A.**, "On the accuracy of benchmark tables and graphical results in the applied mechanics literature", *ASME J. Appl. Mech*, .**69**/1 (2002), 88-90.
15. **Munz, D.** and **Yang, Y.Y.**, "Stresses near the edge of bonded dissimilar materials described by two stress intensity factors", *Int. J. Fracture*, **60** (1993), 169-177.
16. **Seweryn, A.** and **Molski, K.**, "Elastic stress singularities and corresponding generalized stress intensity factors for angular corners under various boundary conditions", *Eng. Frac. Mech.*, **55**/4 (1996), 529-556.
17. **Pageau, S.S., Gadi, K., Biggers, S.B., Jr.** and **Joseph, P.J.**, "Standardized complex and logarithmic eigensolution for n-material wedges and junctions", *Int. J. Fracture*, **77** (1996), 51-76.
18. **Barroso, A., Mantič, V.** and **París, F.**, "Singular stress characterization in anisotropic multimaterial corners involving mathematically degenerate materials: Applications to adhesive joints", *ECCM-10 Conference (CD)*, Brugge (Belgium) (2002).
19. **Barroso, A., Mantič, V.** and **París, F.**, "A general procedure for singularity analysis of anisotropic elastic multimaterial corners. Application to adhesive joints", *44th AIAA Conference (CD)*, Norfolk (USA) (2003).